



Science & Technology  
Facilities Council

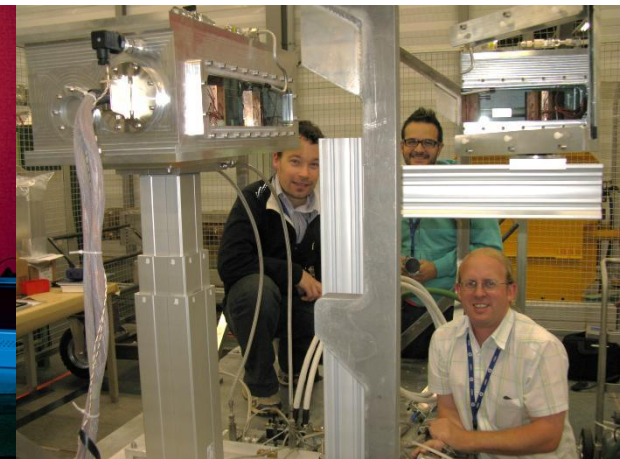
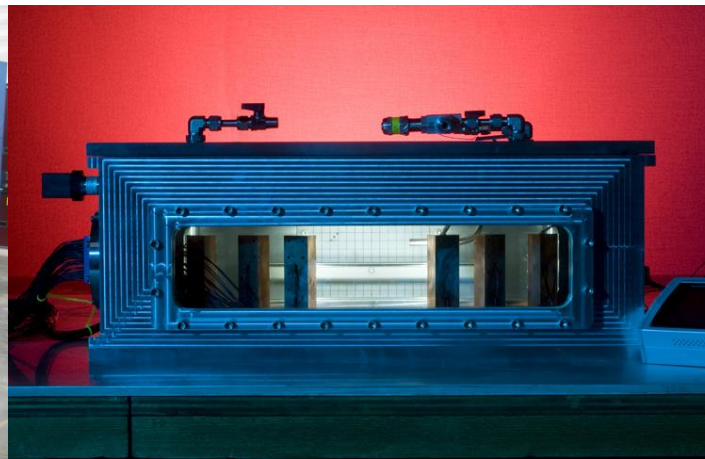
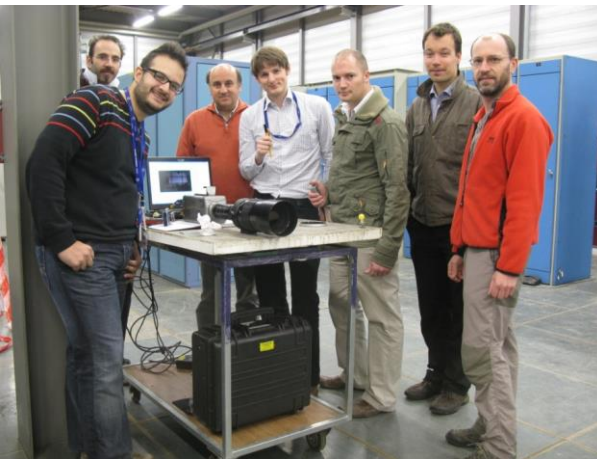
# Tungsten Powder as an accelerator target

Ottone Caretta, Tristan Davenne, Peter Loveridge,  
Rachel Salter, Andrew Atherton, Mike Fitton,  
Joe O'Dell, Dan Wilcox, Scott Bennetton and Chris Densham

(RAL)

Ilias Efthymiopoulos, Nikolaos Charitonidis  
(CERN)

Funded by ASTEC, CERN subscriptions & PASI



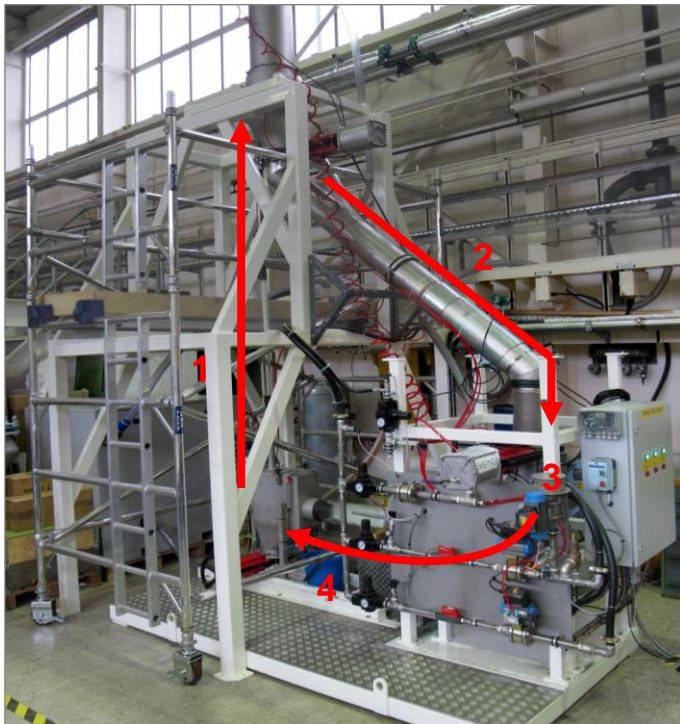
# Tungsten Powder programme live areas of work

- **Rig improvement**
  - CW upgrade
  - Improving the receiver vessel
  - Improving diagnostic
  - Increasing the solid fraction
  - calorimetry
- **In beam tests HiRadMat**
  - Understanding factor/factors for beam powder lift
    - aerodynamic
    - stress propagation
    - Electrostatic
    - a combination of all the above!
- **Understanding fluidisation conditions and pressure loss**

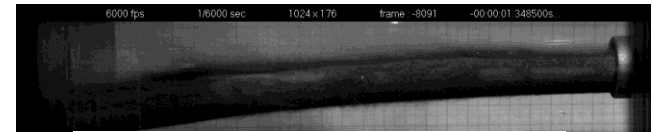


# Tungsten Powder Test Programme in PASI-WP3 + ASTEC

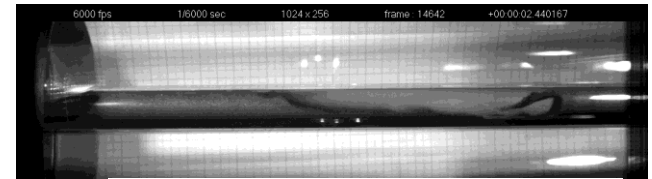
- Offline testing
  - Pneumatic conveying (dense-phase and lean-phase)
  - Containment / erosion
  - Heat transfer and cooling of powder



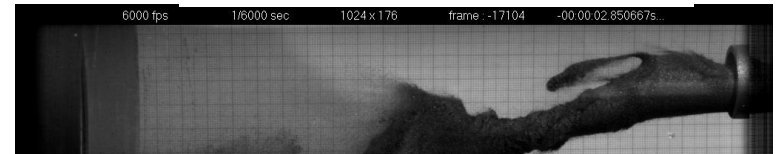
## Dense-phase delivery



*High speed image: tungsten powder jet*

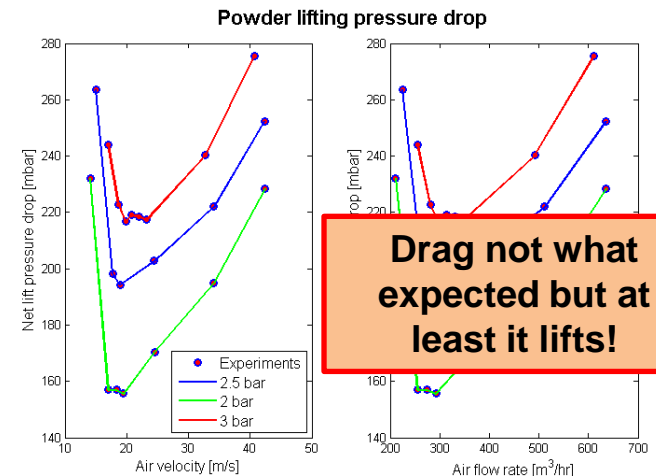


*High speed image: tungsten powder flow in a pipe*

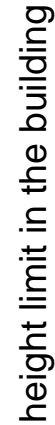


*Unstable tungsten powder jet*

## Lean-phase lift

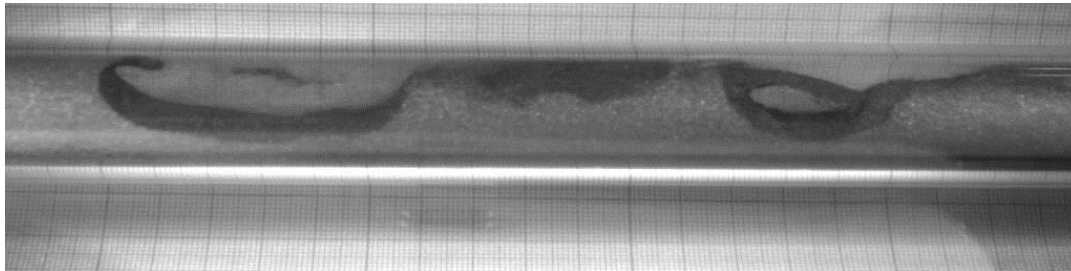
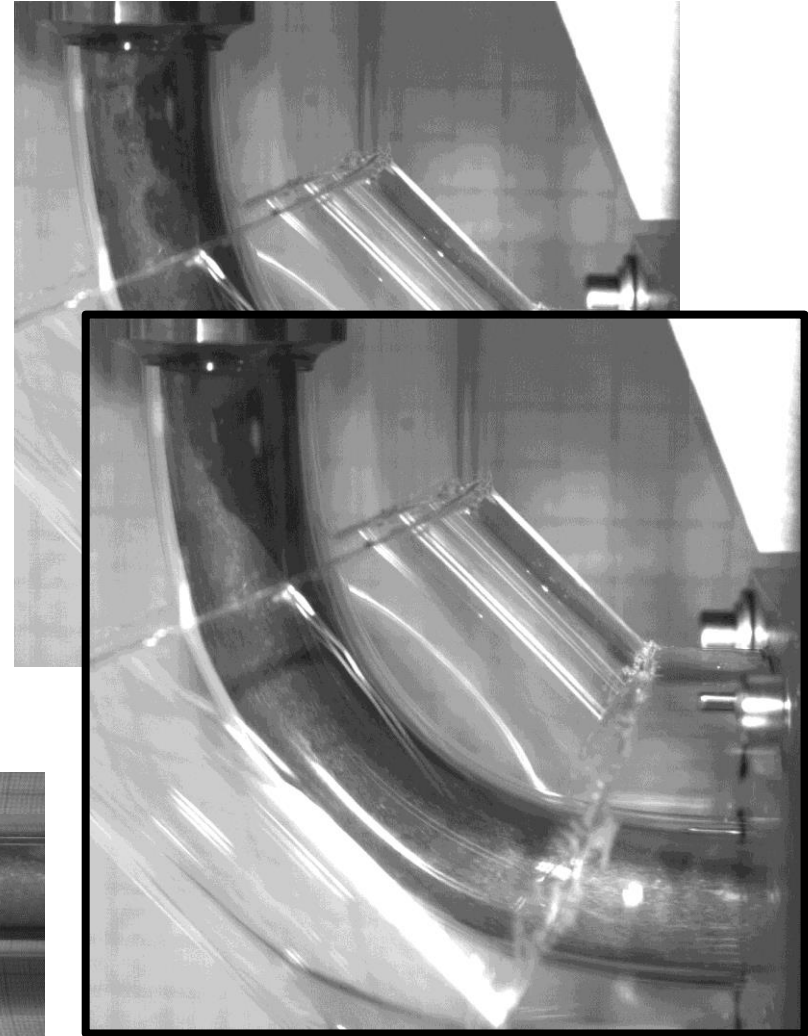


# Dan Wilcox





# Improving diagnostics to increase the solid fraction



New glass parts show early stages of phase separation



Science & Technology Facilities Council  
Rutherford Appleton Laboratory

# Phase separation diagnostic improvement

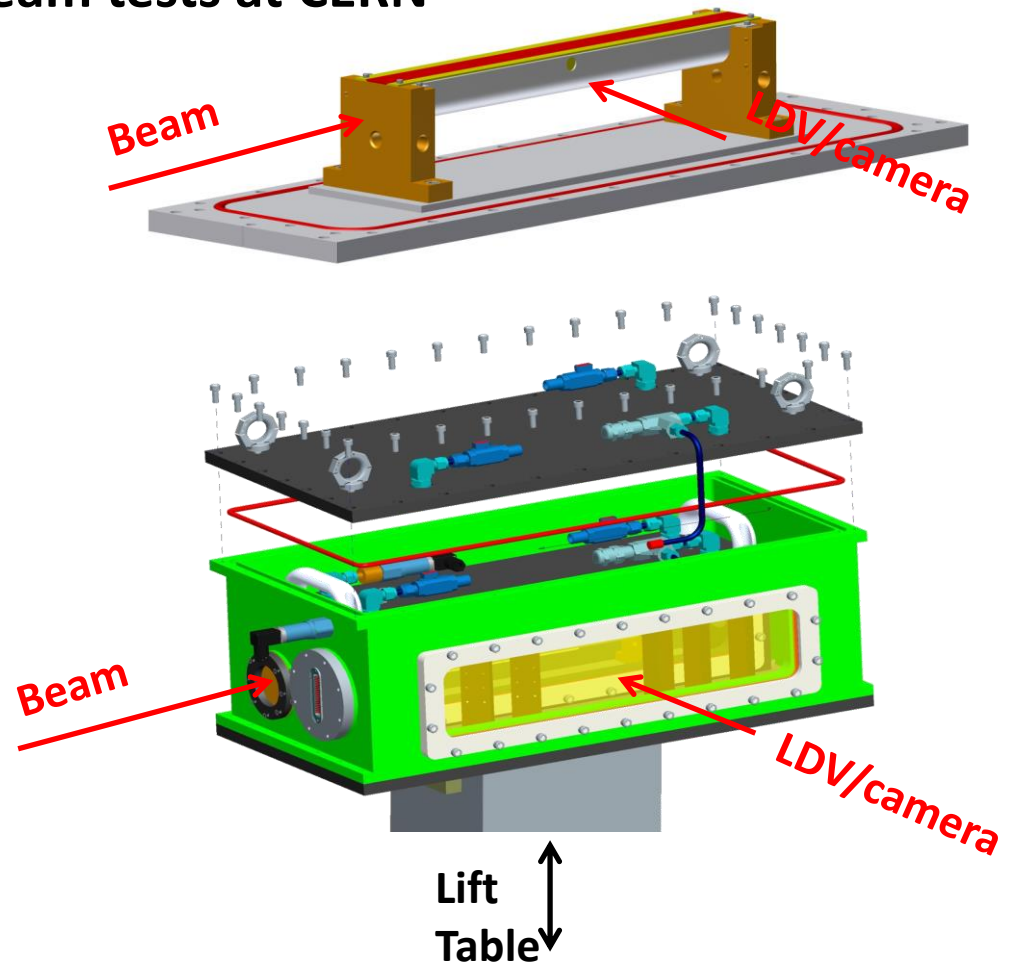
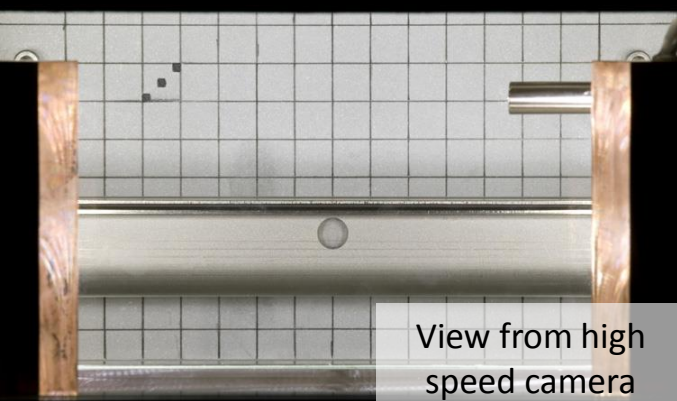
Next stages:

- Vary system characteristic pressure drop (i.e. pipe diameter and length)
- See how the powder flows through the dense phase hopper





## In beam tests at CERN



- Tungsten powder sample in an open trough configuration
- Helium environment
- Two layers of containment with optical windows to view the sample
- Remote diagnostics via LDV and high-speed camera

# Prompt energy deposition/radiation ( FLUKA® Monte – Carlo Code )

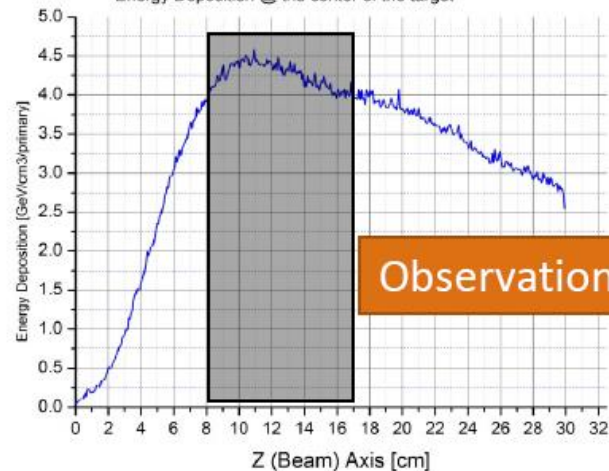
Front

Top

6 mm

Maximum  
Energy Deposition:  
4.5GeV/cm<sup>3</sup>/primary

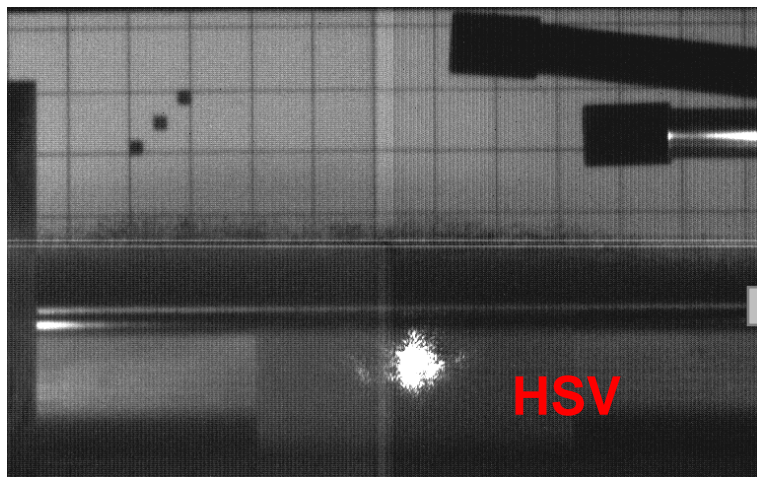
Energy Deposition @ the center of the target



Observation window

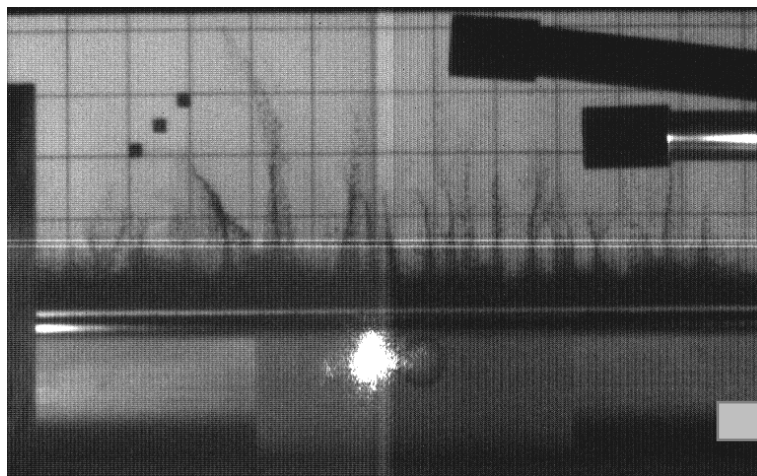
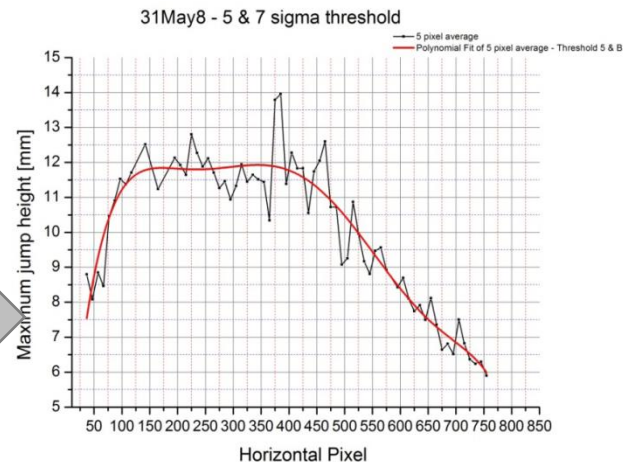


# Charitonidis

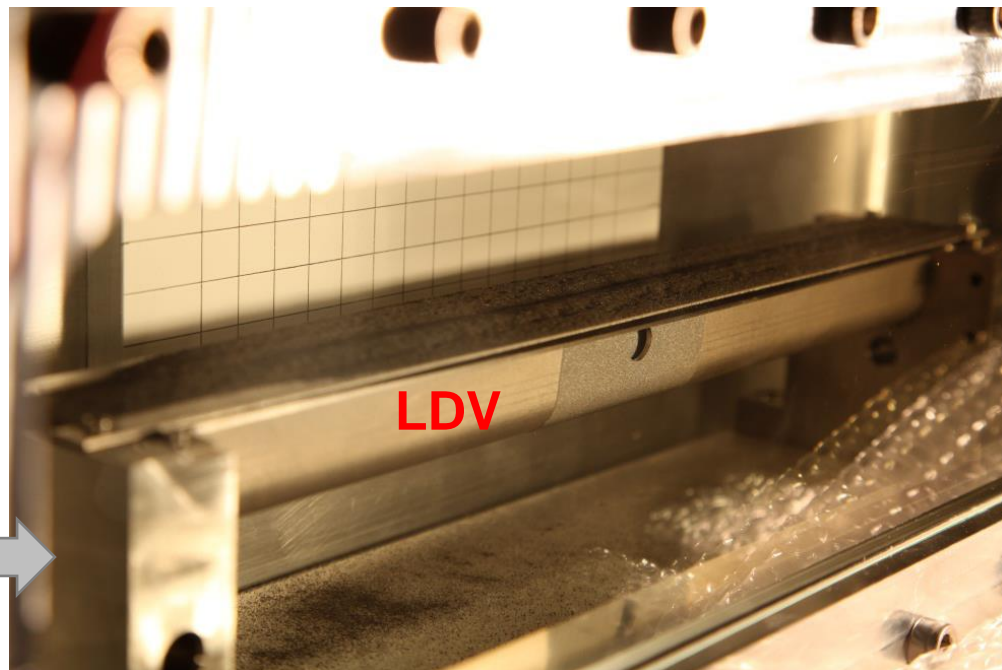


Shot #8,  $1.75 \times 10^{11}$  protons  
Note: nice uniform lift

Lift height  
correlates with  
deposited  
energy



Shot #9,  $1.85 \times 10^{11}$  protons  
Note: filaments!



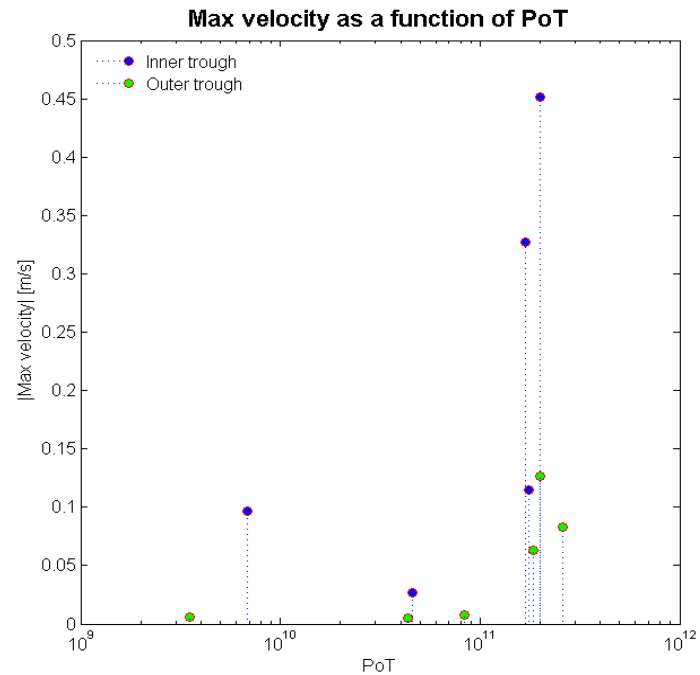
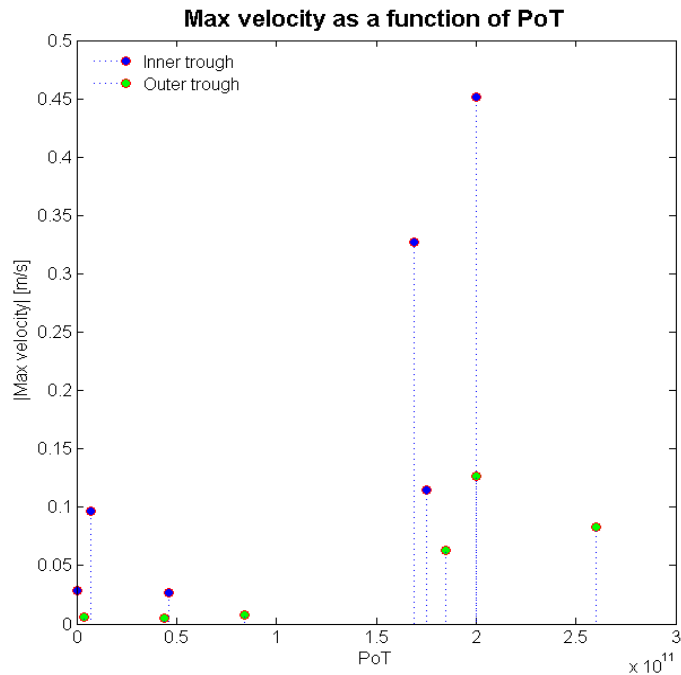
Trough photographed after the experiment.  
Note: powder disruption



# LDV: the good bits

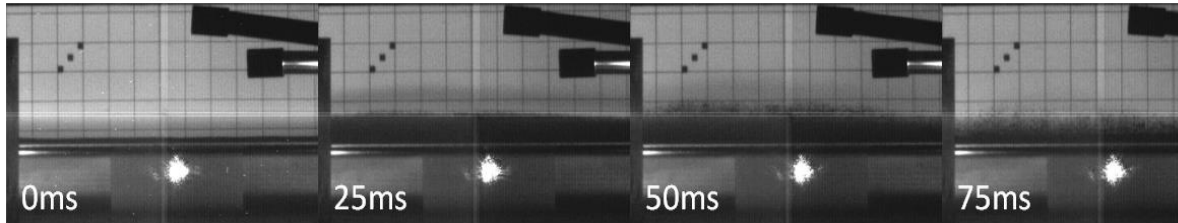
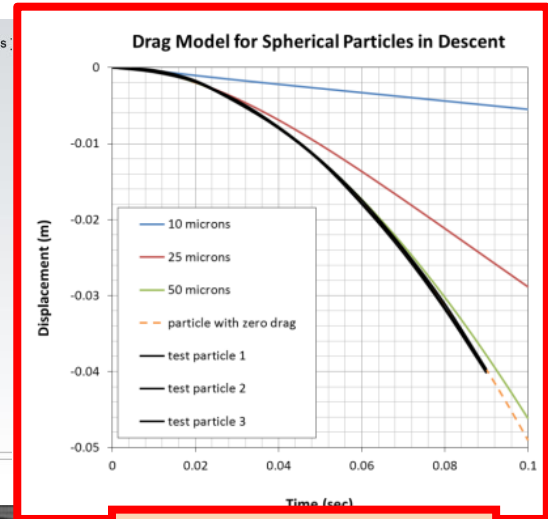
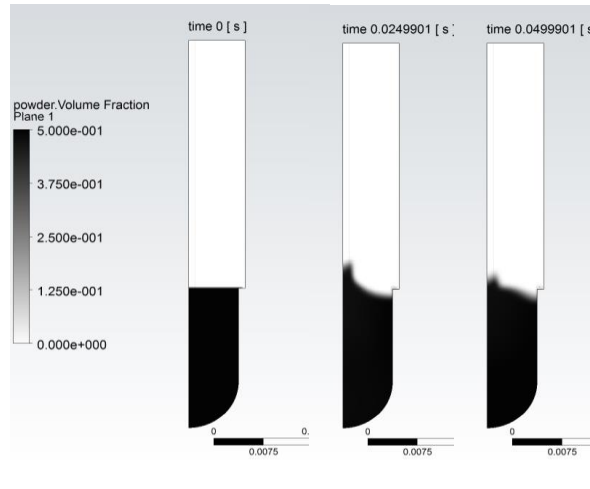
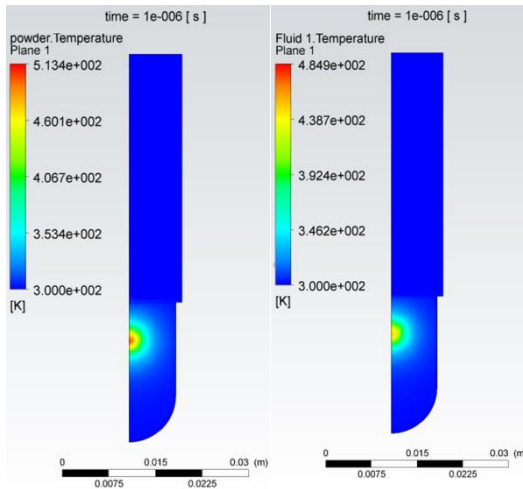
Having taken all the bad data away (technically defined as data massaging!!)

- the amplitude of vibration appears proportional to PoT
- Vibration amplitude is higher in the inner trough than on the outer trough
- There is a 1kHz resonant frequency peak (expected from trough resonance )

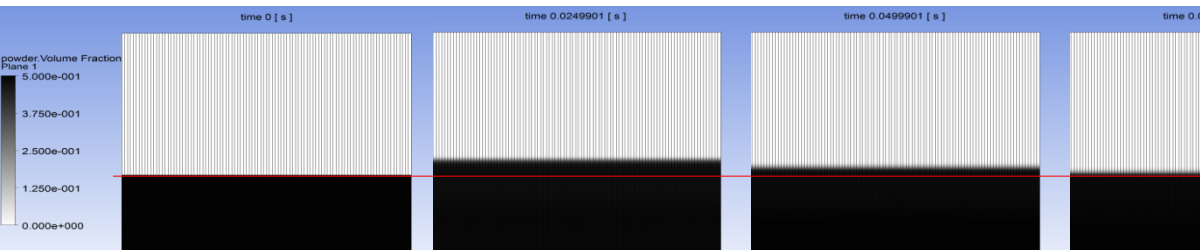


# Davenne: CFD predictions/post fits

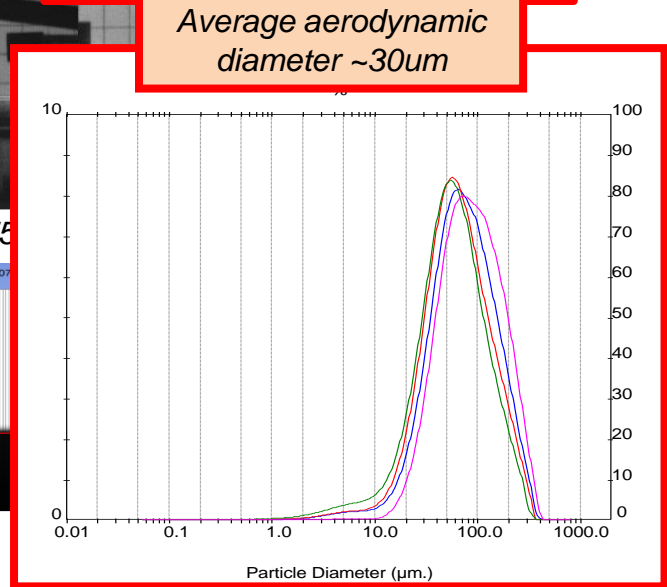
## Beam heating



Test Results from Shot #8,  $1.75 \times 10^{11}$  protons, beam sigma 0.75



CFD simulation of Shot #8, assuming 1 micron particle size  
(n.b. no lift with 25 micron particles at this intensity)





# Powder lift didn't match expectations..

## So looking at the powder falling: Drag coefficient calculations

### Appendix 1: Drag and equations of motion

D: drag force

Re: Reynolds number

$C_d$ : Drag coefficient

v: Particle velocity

$\rho$ : density of fluid

$\mu$ : viscosity of fluid

d: diameter of particle

a: acceleration of particle

x: displacement of particle from peak height

t: time

m: particle mass

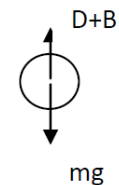
B: Buoyancy

$\rho_p$ : particle density

a: acceleration

$$Re = \frac{\rho v d}{\mu}$$

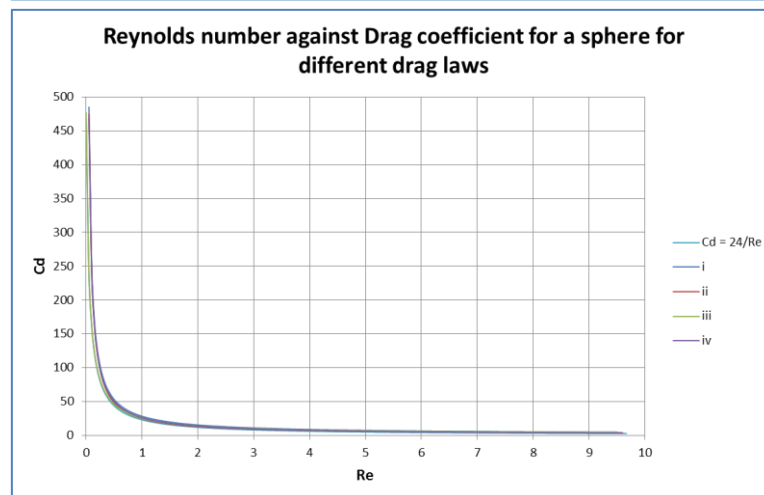
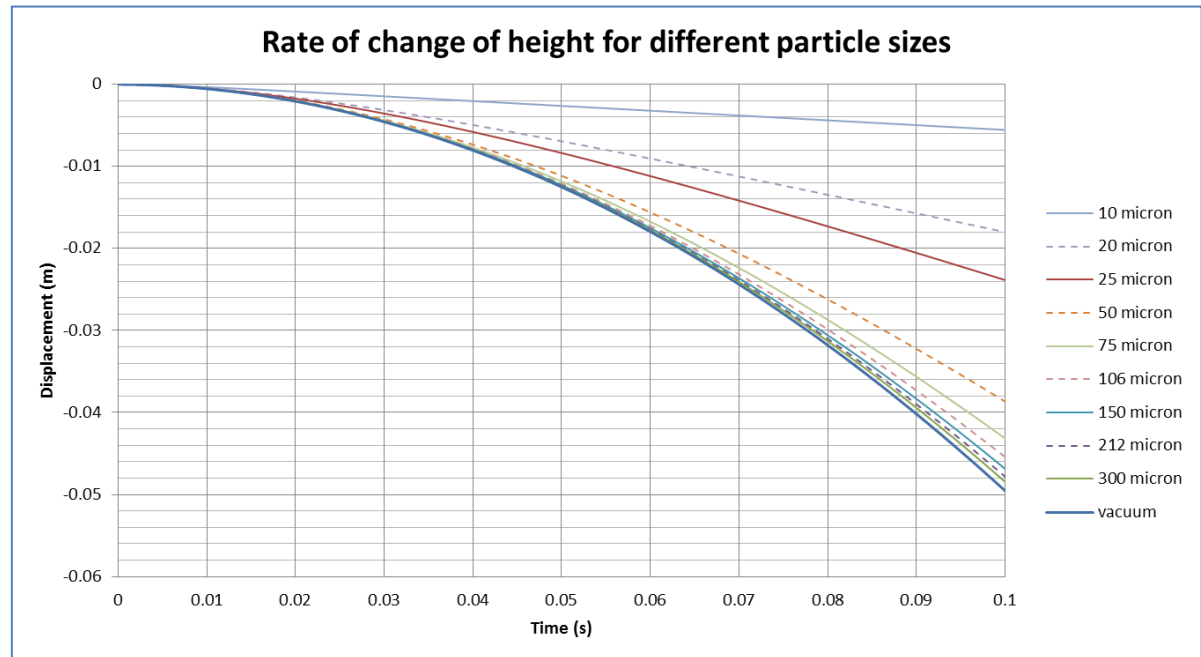
$$D = \frac{\rho v^2 \pi d^2 C_d}{8}$$



$$B = \frac{m \rho a}{\rho_p}$$

$$D + B - mg = ma \text{ (defining up as positive)}$$

$$x = vt + 0.5at^2$$



i)  $C_d = \frac{24}{Re} + \frac{4}{Re^{0.32}}$  (valid for  $1 < Re < 1000$ ) (Ahmadi)

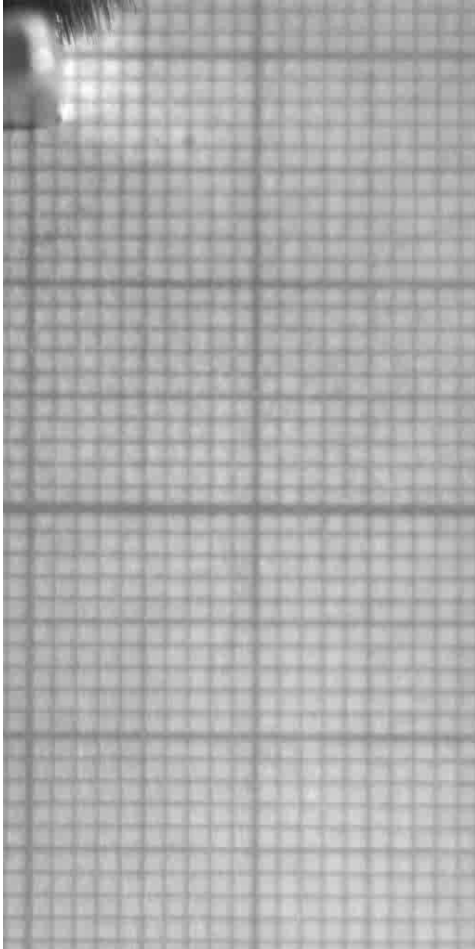
ii)  $C_d = \frac{24}{Re} + \frac{(2.6 \times \frac{Re}{0.5})}{1 + (\frac{Re}{5})^{1.52}}$  (there are two further terms that were considered negligible when investigating low Reynolds number) (Morrison, 2013)

iii)  $C_d = \frac{24}{Re} \left(1 + \frac{3}{16} Re\right)^{0.5}$  (for  $Re < 100$ ) (Massey, 1989)

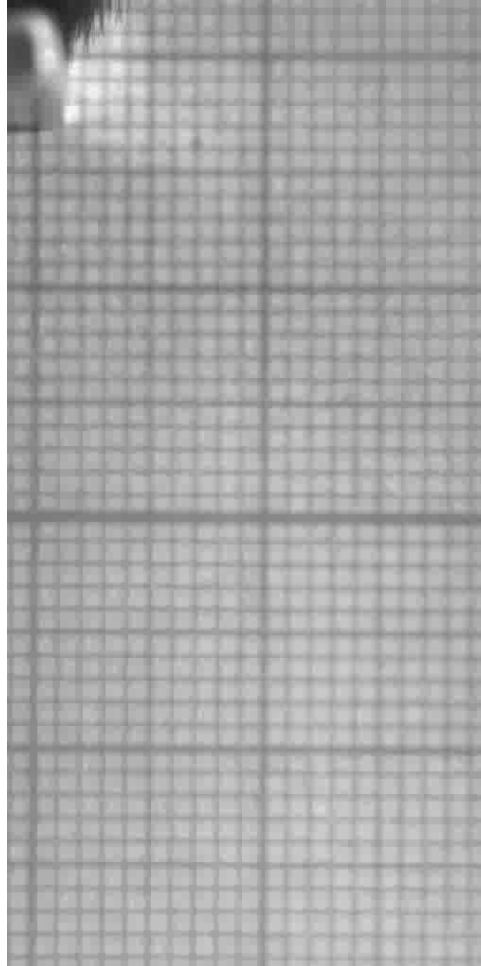
iv)  $C_d = \left(0.63 + \frac{4.8}{Re^{0.5}}\right)^2$  (used by previous summer student (Gibilaro, 2001))



# Tungsten powder drop tests



Particle size: 50 to 75 um



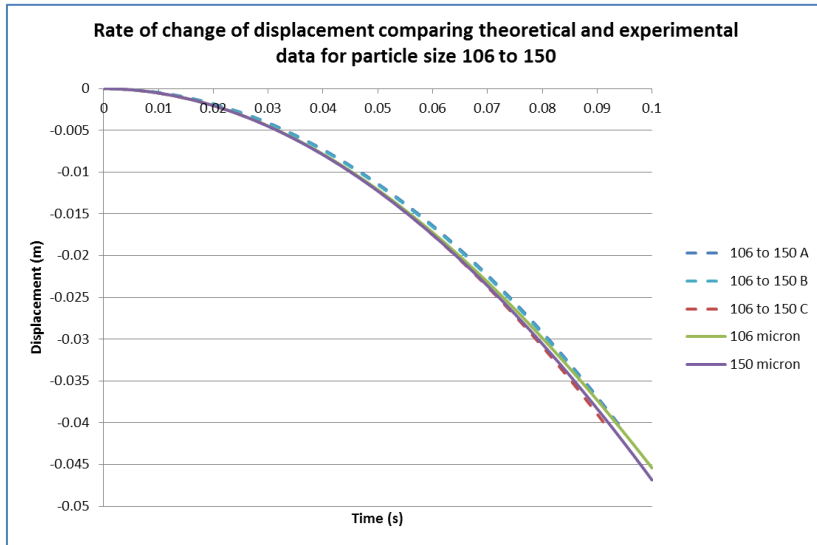
Particle size: 0 to 50 um

Agglomerates only appear to form when there are particles smaller than 50 microns present

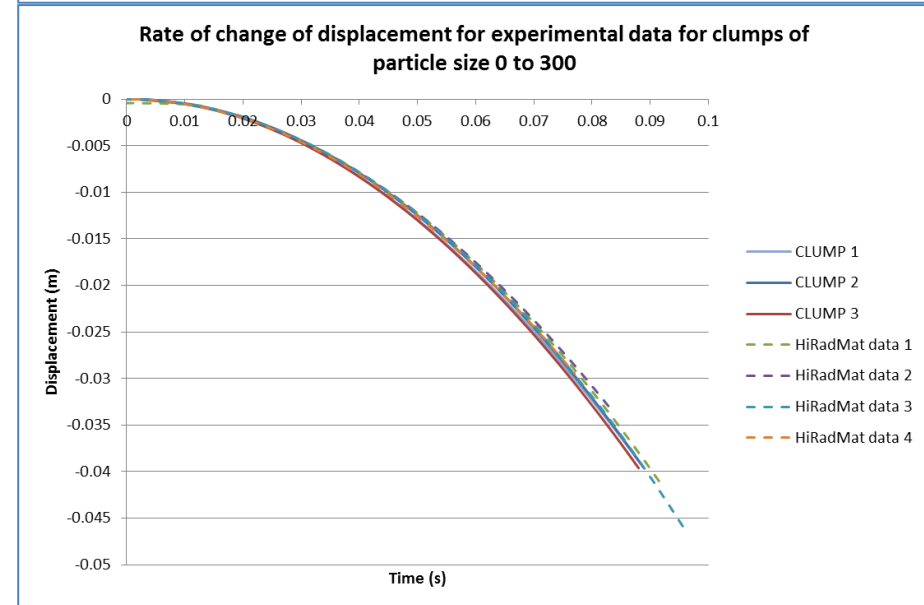
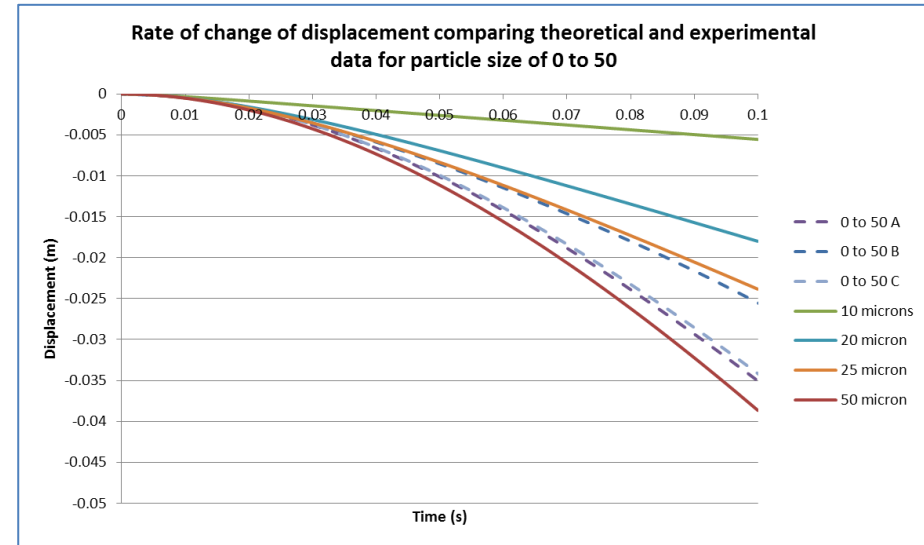
- **Geldart Group C** particles
- For Tungsten powder, **20 microns** is the estimated threshold size for agglomeration



# Tungsten powder drop tests (2)



- Theoretical data fits quite closely to data obtained by tracking single particles- **drag equations** are therefore justified using **spherical** assumption
- HiRadMat data follows a similar trend to agglomerates tracked in the powder drop test- therefore more likely that **clumps of particles** were being tracked





## Tungsten powder puff experiment. Trying to understand the powder lift

piston

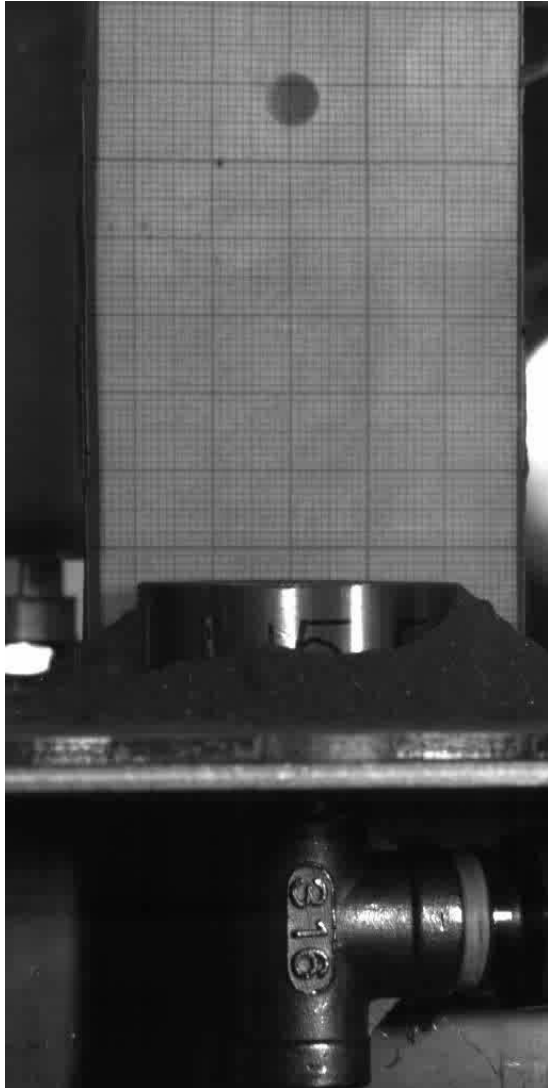
Puff cell



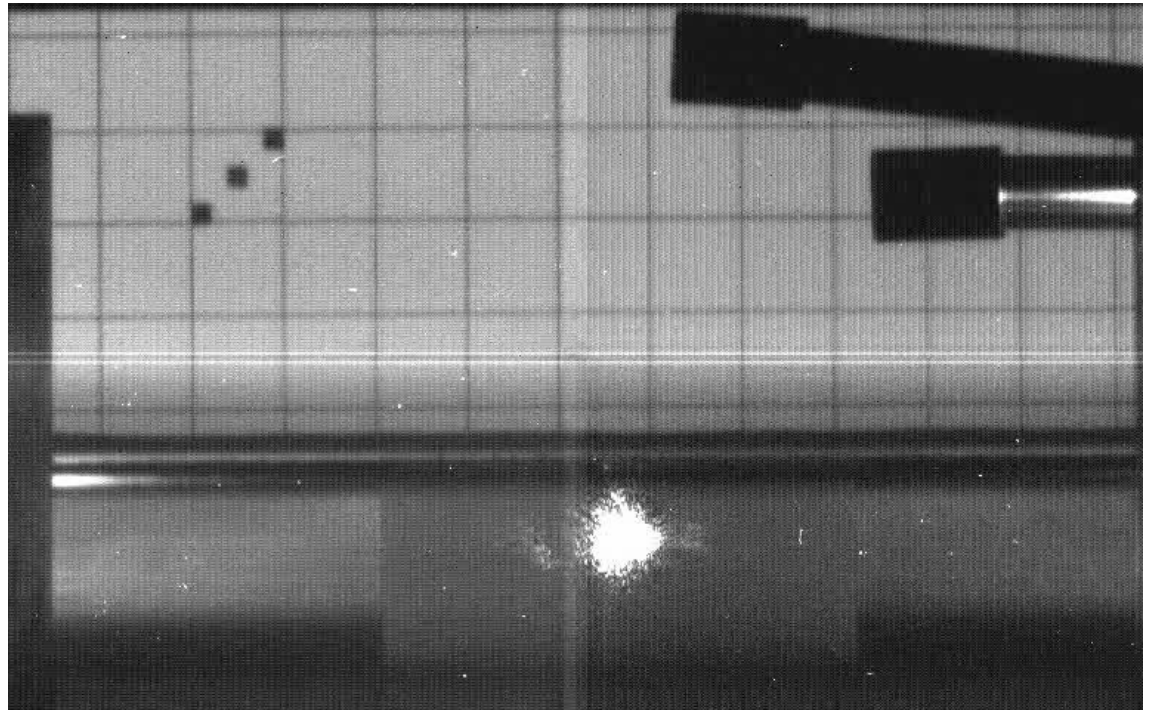
Science & Technology Facilities Council

Rutherford Appleton Laboratory

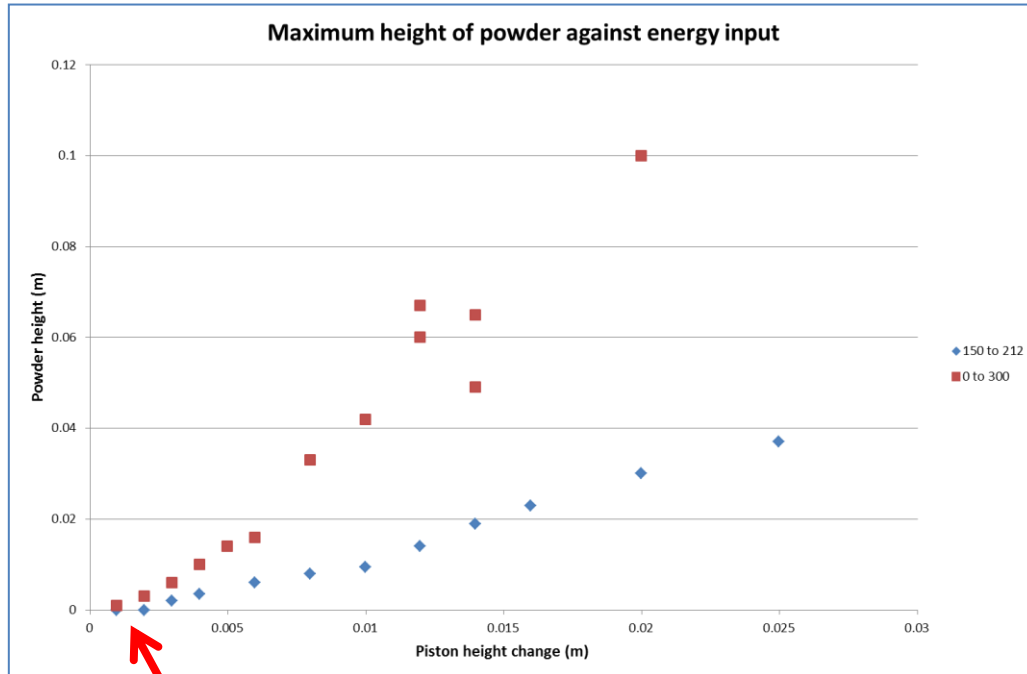
# Tungsten powder puff experiment



- Aim: To compare behaviour of Tungsten powder after a short pressure spike against the behaviour in the HiRadMat experiment
- Method: Use a short pressure pulse to lift the powder



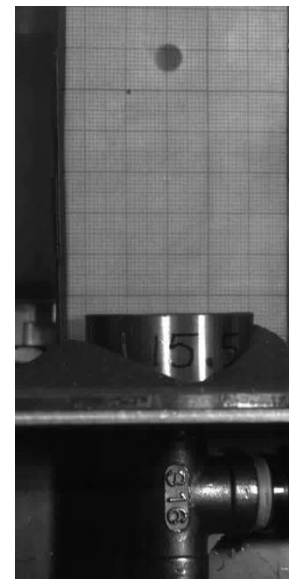
# Tungsten powder puff experiment (2)



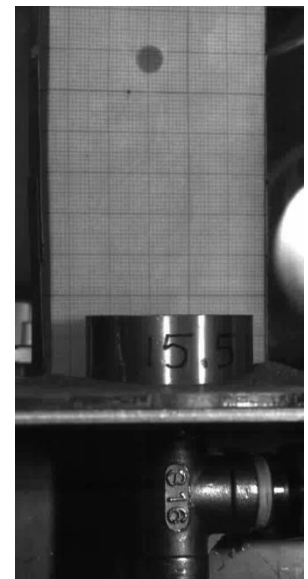
There is a threshold energy which has to be reached before the powder begins to lift. The threshold depends on the depth of the powder

- The maximum height reached by the powder is proportional to the energy put in by the compression of the piston
- The powder sample containing smaller particles was lifted higher than the sample containing only larger particles
- The acceleration is faster than can be captured with 1kHz HSV

0 to 300 um



150 to 212 um





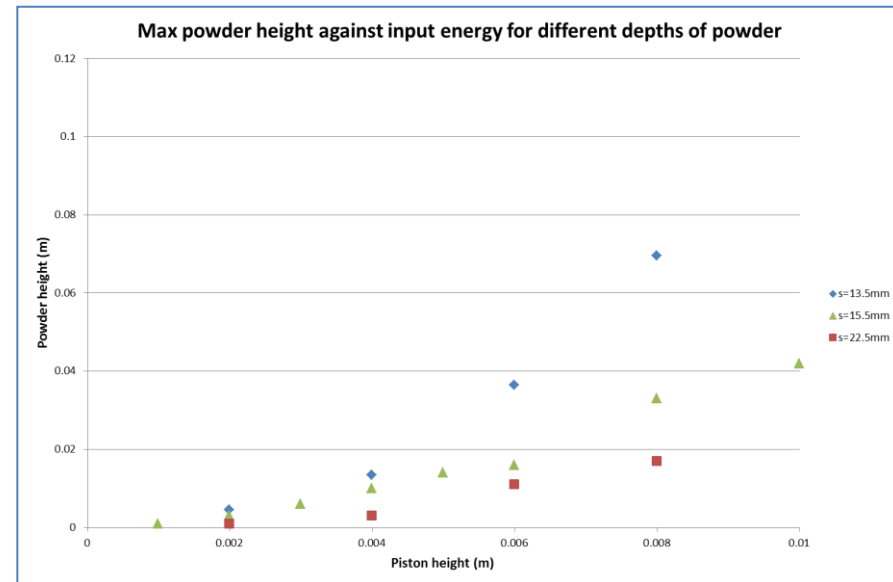
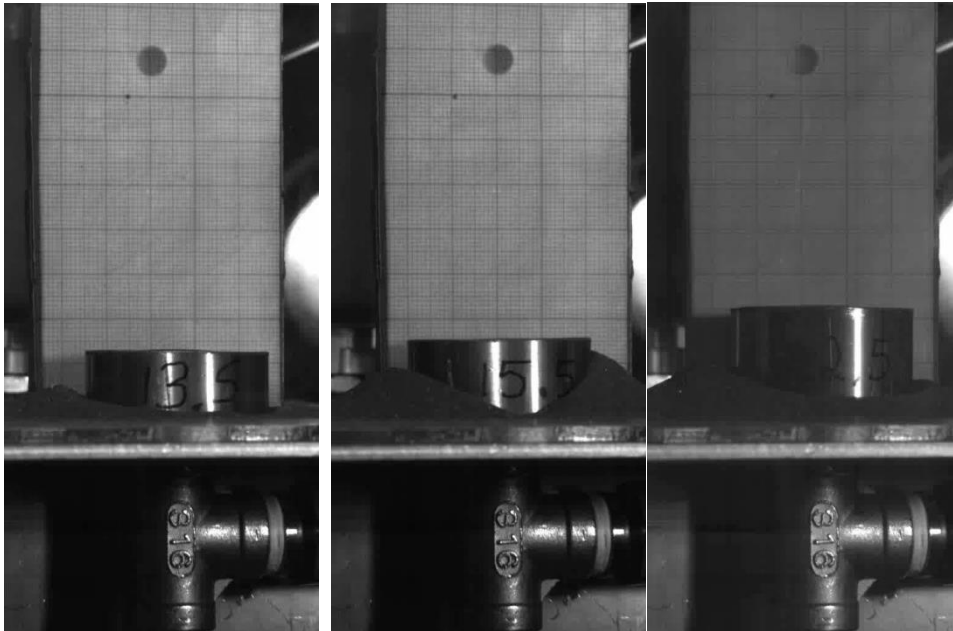
# Tungsten powder puff experiment (3)

Powder depth  
= 13.5mm

Powder depth  
= 15.5mm

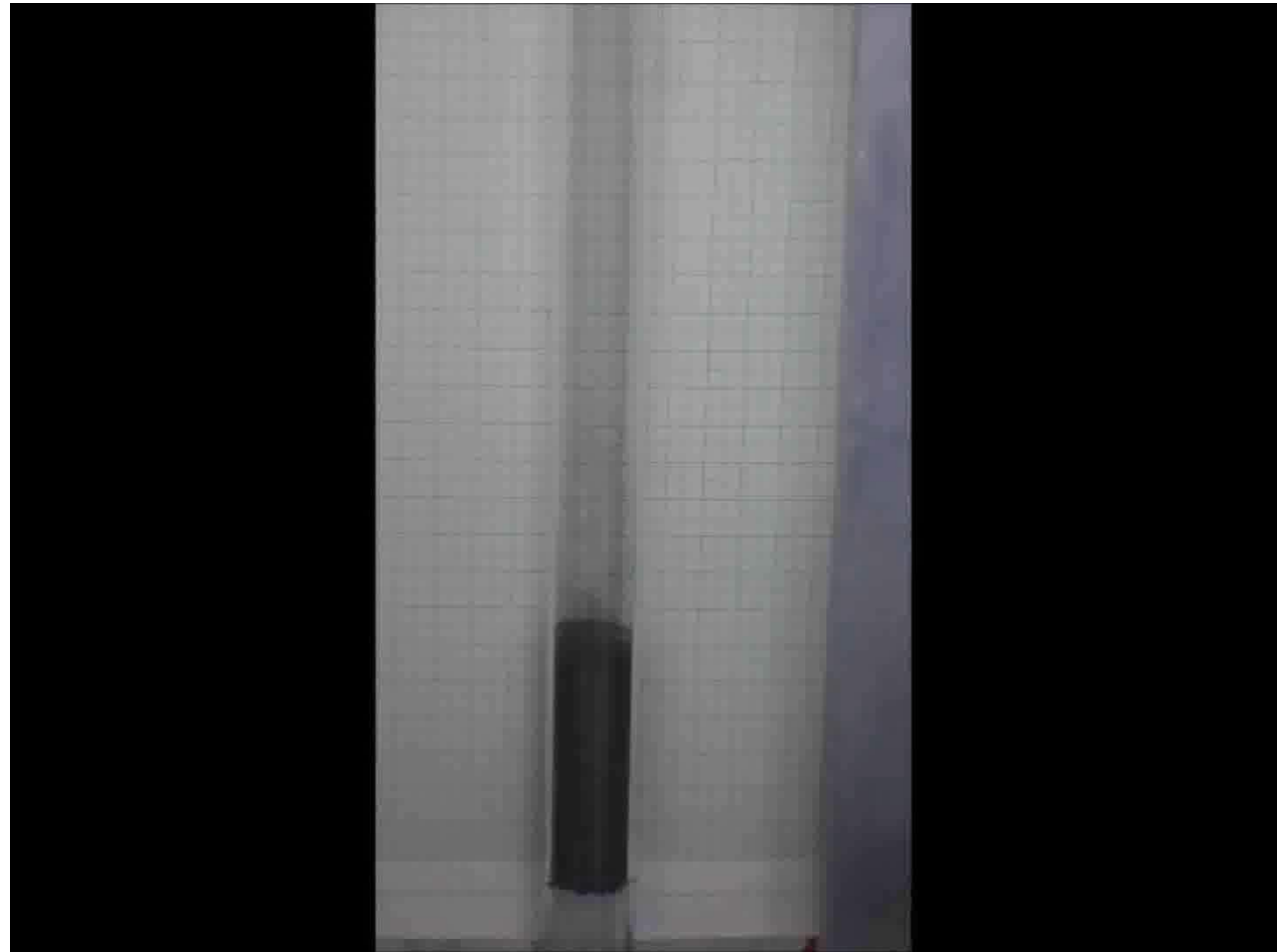
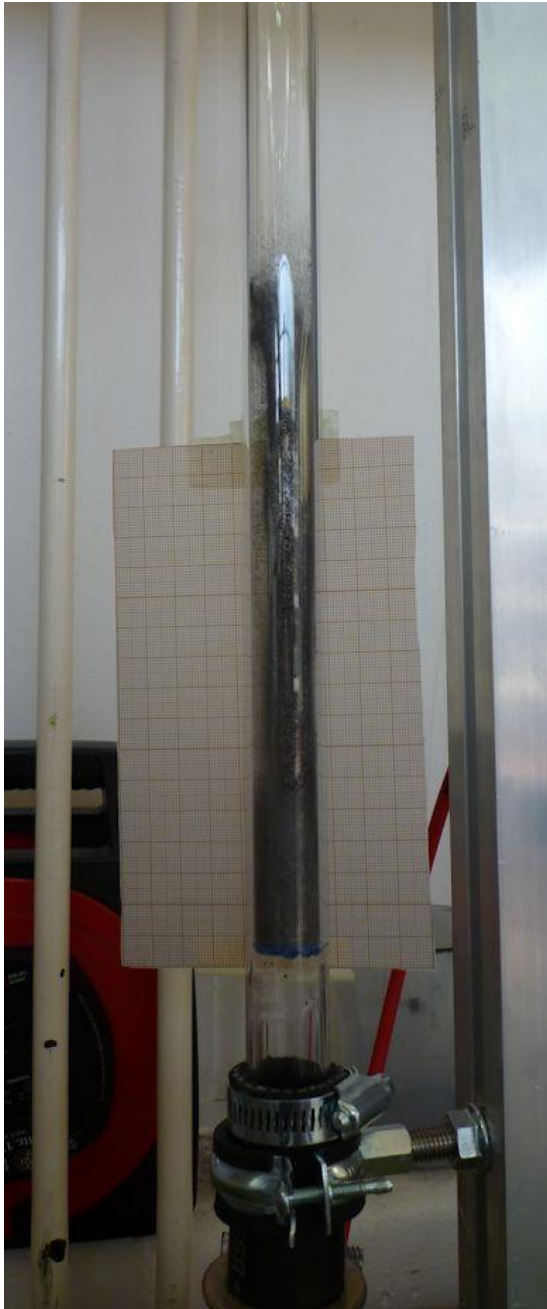
Powder depth  
= 22.5mm

- The smaller the depth of powder, the larger the maximum powder height reached



## Understanding powder lift part 2

Pressure drop for air flowing through a bed of powder



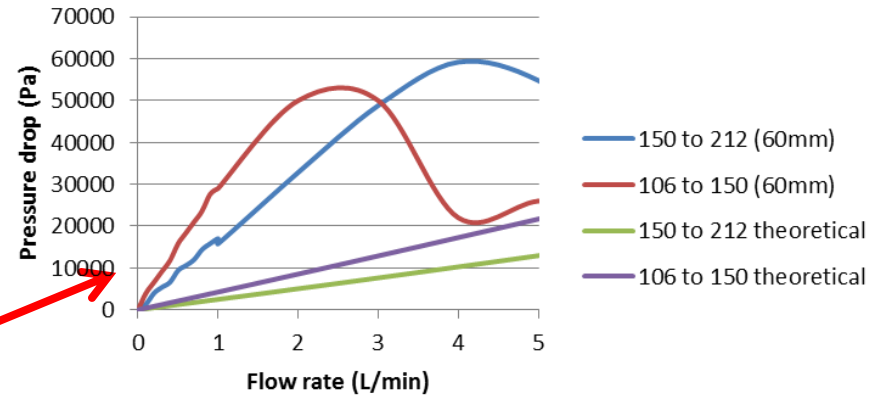
# Fluidised bed experiment (2)

- The experimental change in pressure is consistently much larger than the expected change
- Theoretical calculations rely heavily on **shape factor** ( $\psi$ ) and **void fraction** ( $\epsilon$ ), and are usually applied to much **less dense** material

$$\frac{\Delta P}{h} = \rho_g U^2 \left[ \frac{150(1-\epsilon)}{Re_d \psi} + \frac{7}{4} \right] \frac{1-\epsilon}{\psi d_p \epsilon^3}$$

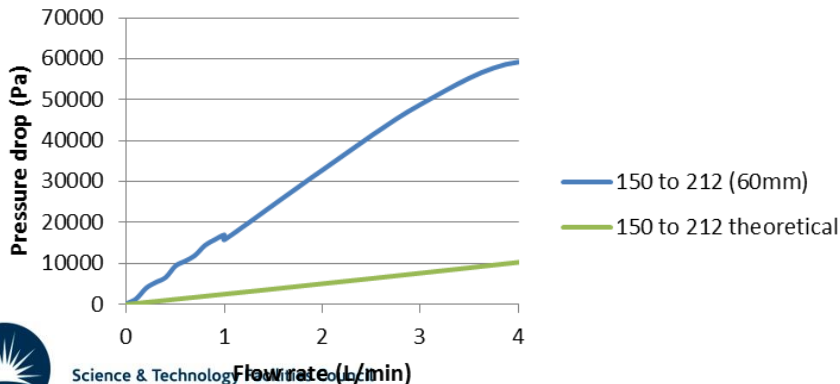
Linear region corresponds to regime before fluidisation has started

Comparison of different powder sizes at a powder depth of 60mm

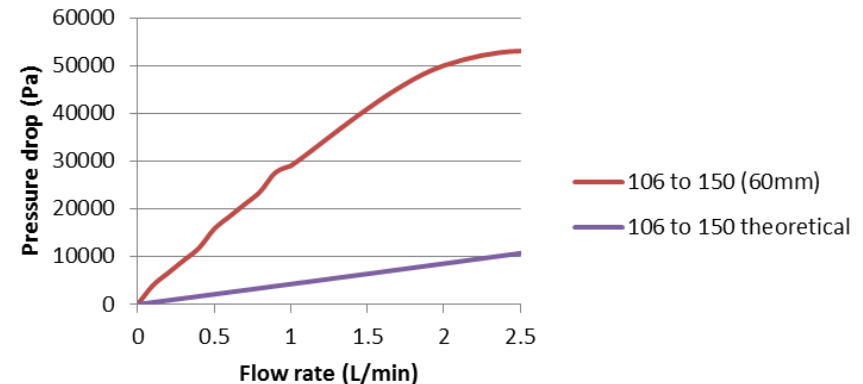


Both Ergun and Carman-Kozeny equations largely underestimate pressure drop

Comparison of different powder sizes at a powder depth of 60mm



Comparison of different powder sizes at a powder depth of 60mm





# Future work to understand W powder dynamics

- Studying the effect of sphericity on flowability and on pressure drop
- Validating the fluidisation experiments on a lighter material (e.g. Glass)
- Investigating electrostatic effects

